PLASMA ASTRO

MAX-PLANCK-INSTITUT FÜR PLASMAPHYSIK

Particle acceleration and high-energy emission in AGN jets: M87 and Cen A

Jieshuang Wang

Max Planck Institute for Plasma Physics (IPP)

Ack: Brian Reville (MPIK), Zigao Dai (USTC), Frank Rieger (IPP), Felix Aharonian (DIAS & MPIK), Yosuke Mizuno (SJTU)

Quasi-continuous radiation along the jet

- M87: multi-wavelength observation resolving sub-pc and kpc scales
- Cen A: most nearby radio galaxies, radio to TeV observations on kpc-scale jets

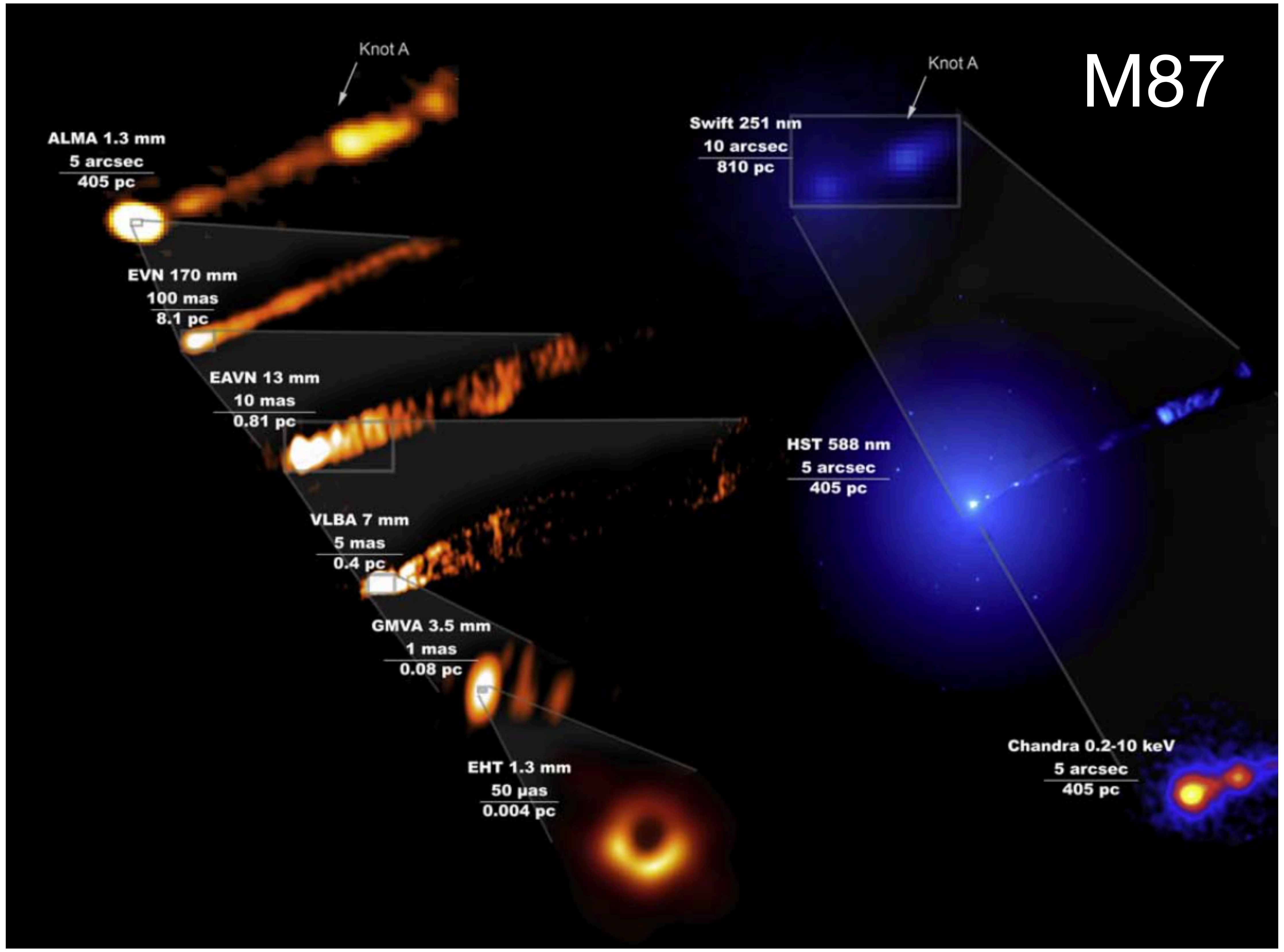

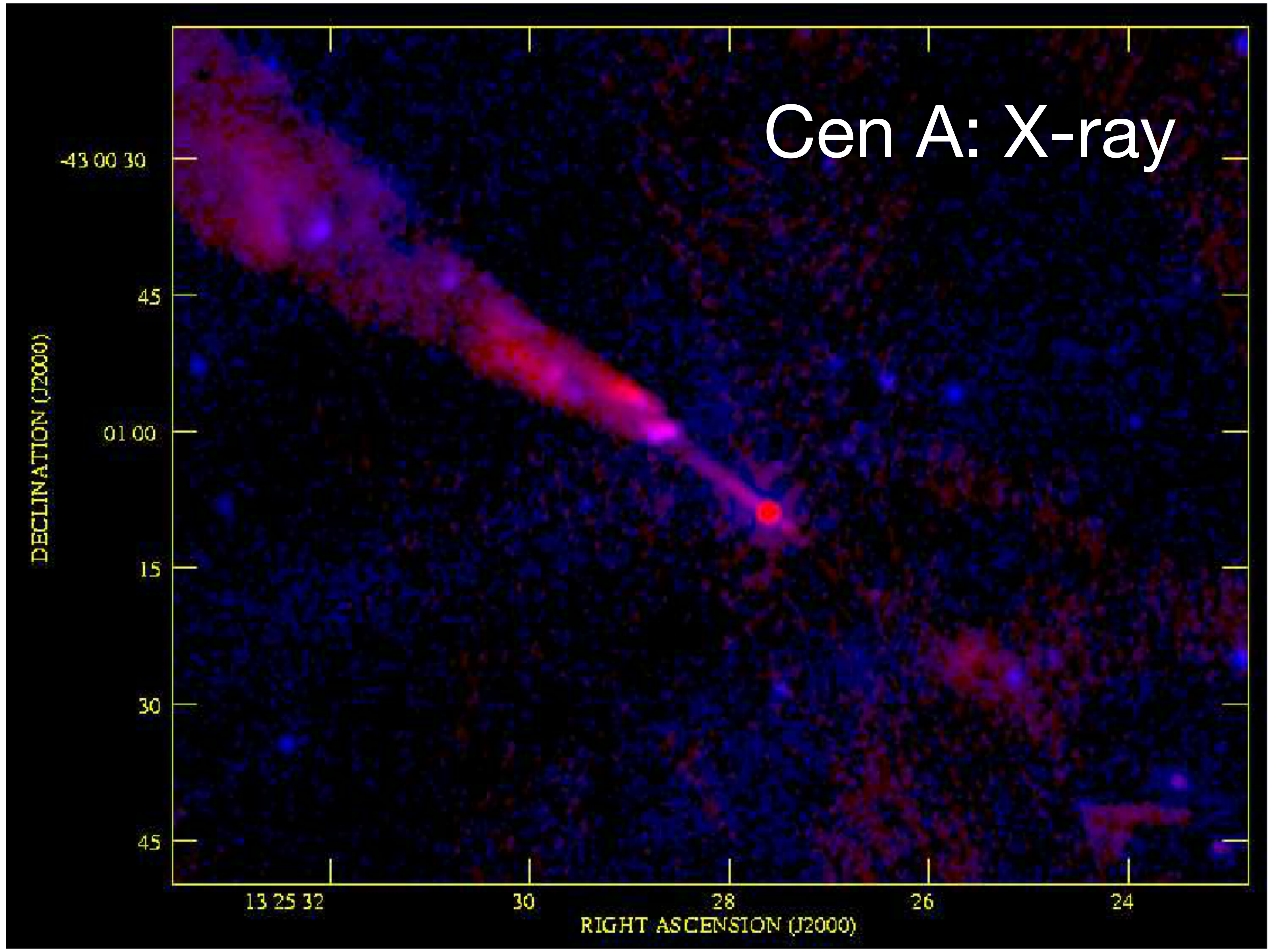

Continuous particle acceleration

- Continuous particle acceleration offers a natural explanation to continuous emission
- In turbulent jet flows, continuous acceleration by Fermi II mechanism
- In spine-sheath flows, continuous acceleration by shear acceleration
- Shock and magnetic reconnection in highly magnetized regions can produce more localized features (e.g. knots, hotspots) and add to the turbulence development

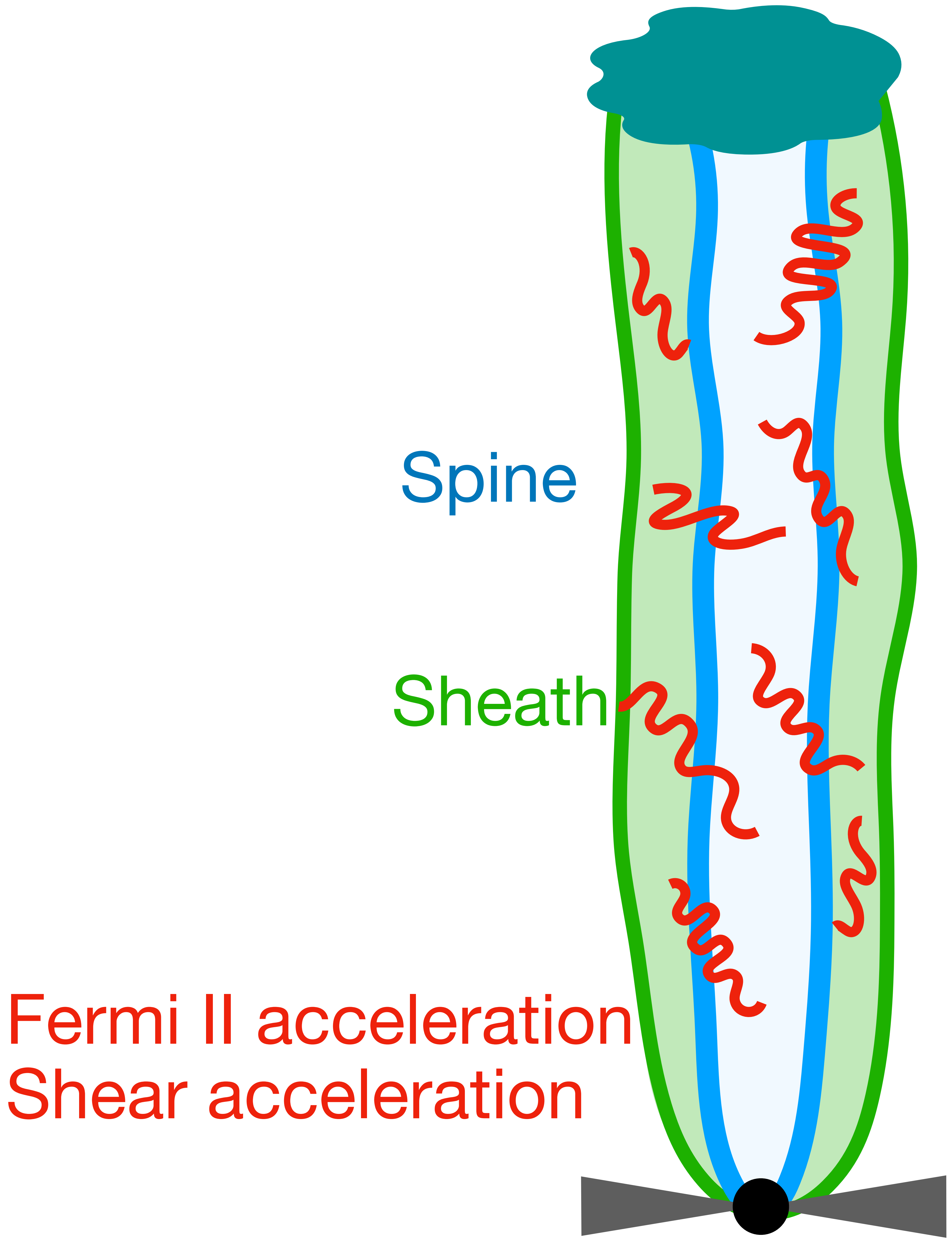

Fermi-II mechanism

- Average energy gain in each collision by scattering MHD waves ($u = v_A = B/\sqrt{4\pi\rho}$)

$$\frac{\langle \Delta\epsilon \rangle}{\epsilon} \propto \left(\frac{u}{c}\right)^2$$

- Scattering time: $\tau_{\rm sc} \propto \epsilon^{2-q}$ (turbulence index q)
- Acceleration time:

$$\tau_{\rm FermiII} = \frac{\epsilon}{< \Delta\epsilon >}\tau_{sc}$$

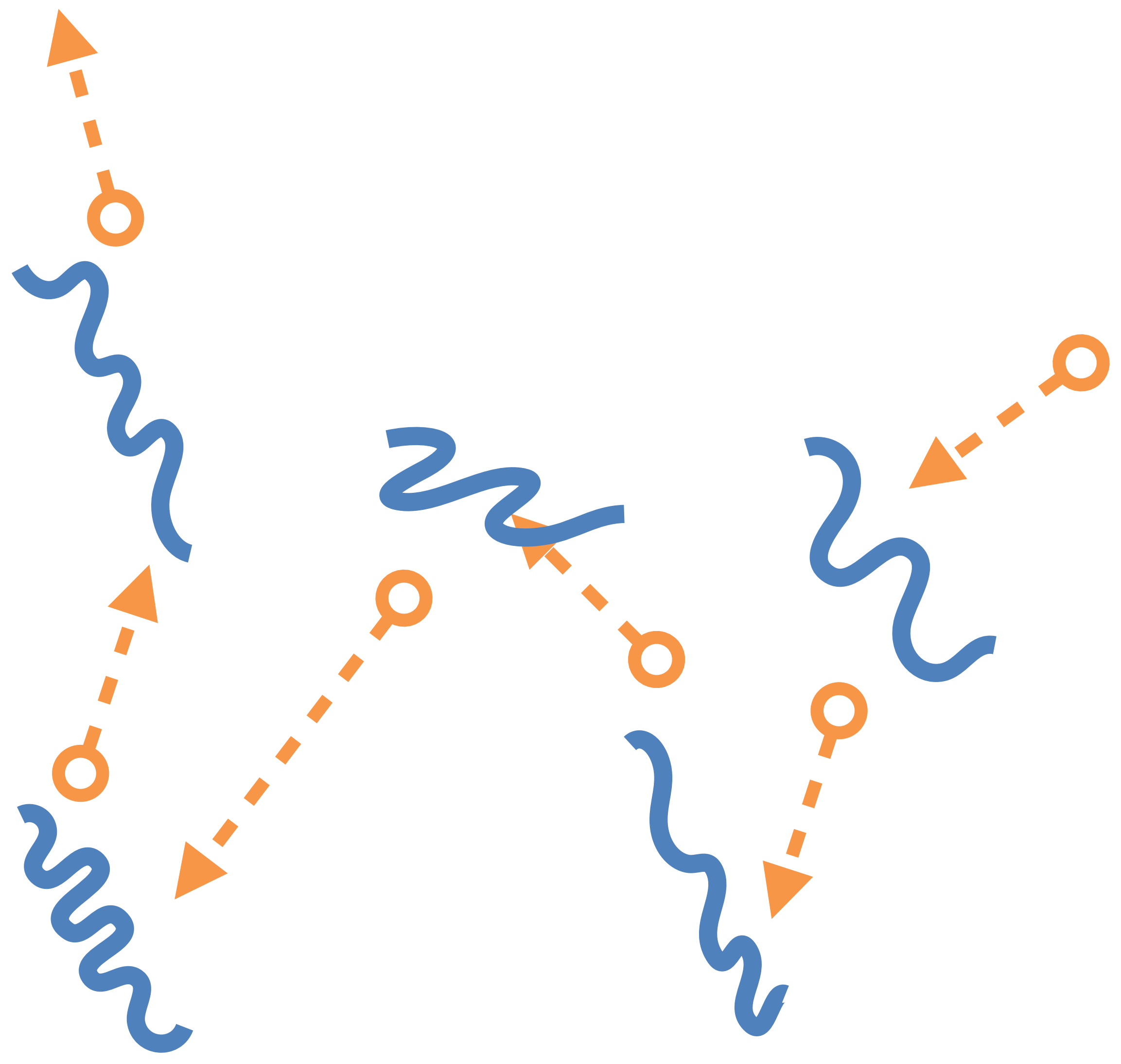

Shear acceleration

- Average energy gain in each collision by scattering MHD waves ($u = v_A = B/\sqrt{4\pi\rho}$)

$$\frac{\langle\Delta\epsilon\rangle}{\epsilon} \propto \left(\frac{u}{c}\right)^2$$

- Scattering time: $\tau_{\rm sc} \propto \epsilon^{2-q}$ (turbulence index q)
- Acceleration time:

$$\tau_{\rm FermiII} = \frac{\epsilon}{< \Delta\epsilon >}\tau_{sc}$$

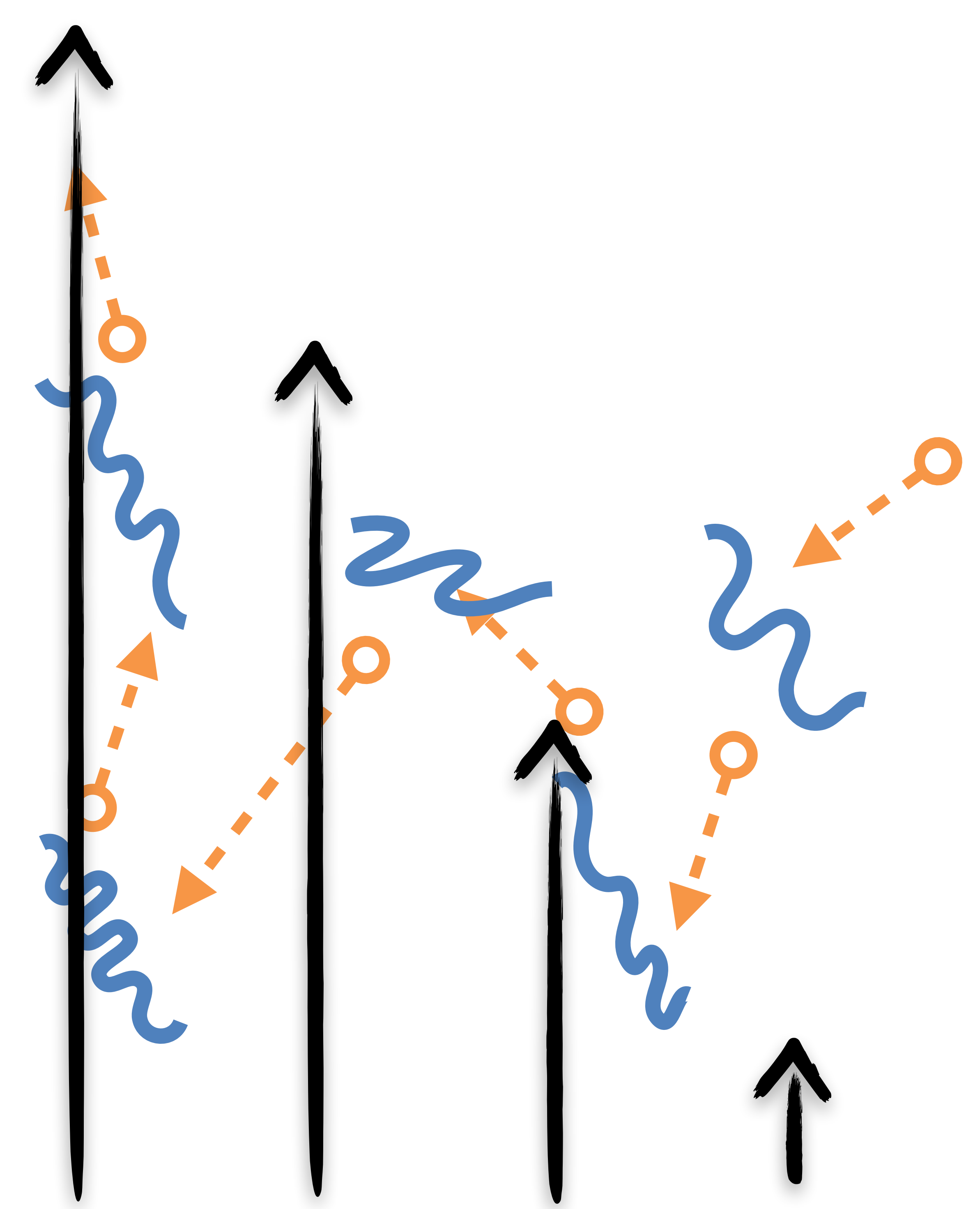

- Shear is also stochastic-type
- Turbulences are embedded in velocity-shearing layers (spine-sheath)
- Particles scattering off turbulence will sample the velocity difference

$$\frac{\langle\Delta\epsilon\rangle}{\epsilon} \propto \left(\frac{\bar{u}}{c}\right)^2 \propto \left(\frac{\partial u_z}{\partial x}\right)^2 \tau_{\rm sc}^2$$

$$\tau_{\rm shear} = \frac{\epsilon}{< \Delta\epsilon >}\tau_{\rm sc}$$

Berezhko & Krymsky 1981; Berezhko 1982; Earl+ 1988; Webb 1989; Jokipii & Morfill 1990; Webb+ 1994; Rieger & Duffy 2004, 2006, 2016; Liu+ 2017; Webb+ 2018, 2019; Lemoine 2019; Rieger & Duffy 2019, 2021,2022

Analytical solution for Stochastic-type acceleration

- Fokker–Planck description for particle spectrum (steady state)

$$\frac{\partial n(\gamma,t)}{\partial t}=\frac{1}{2}\frac{\partial}{\partial\gamma}\left[\left\langle\frac{\Delta\gamma^2}{\Delta t}\right\rangle\frac{\partial n(\gamma,t)}{\partial\gamma}\right]-\frac{\partial}{\partial\gamma}\left[\left(\left\langle\frac{\Delta\gamma}{\Delta t}\right\rangle-\frac{1}{2}\frac{\partial}{\partial\gamma}\left\langle\frac{\Delta\gamma^2}{\Delta t}\right\rangle+\langle\dot{\gamma}_c\rangle\right)\times n(\gamma,t)\right]-\frac{n}{t_{\rm esc}}+Q(\gamma,t)$$

- Cutoff power-law spectrum for both mechanism: turbulence, magnetic field (B), jet velocity (v) and profile

Fermi II: $N(\gamma')\propto\gamma'^{-p}\exp[-(\frac{\gamma'}{\gamma'_{\rm cut,Fermi-II}})^{3-q}]$ $\quad p_{\rm Fermi-II}=q-1$

Cutoff frequency: $\nu'_{\rm cut,Fermi-II}=2.9\times10^4\beta'^3_{A,-1}\zeta^{3/2}_{-2}B'^{-3/2}_{-1}R^{-1}_{-2}$ GHz

Shear: $n(\gamma')\propto\gamma'^{s_-}F_-(\gamma',q)+C\gamma'^{s_+}F_+(\gamma',q)$ $\quad s_\pm=\frac{q-1}{2}\pm\sqrt{\frac{(5-q)^2}{4}+w}$

Cutoff frequency: $\nu'_{\rm cut,sh}=2.4\times10^9w^{-3}_{-1}\zeta^{-3}_{-2}B'^{-6}_{-1}R^{-4}_{-2}$ GHz $\quad w=\frac{10c^2}{\Gamma^4(r)R^2}\left(\frac{\partial u(r)}{\partial r}\right)^{-2}$

J.S.Wang+, 2021, arXiv:2105.08600, 2024, arXiv:2404.08625

Observed profiles for the M87 inner jet

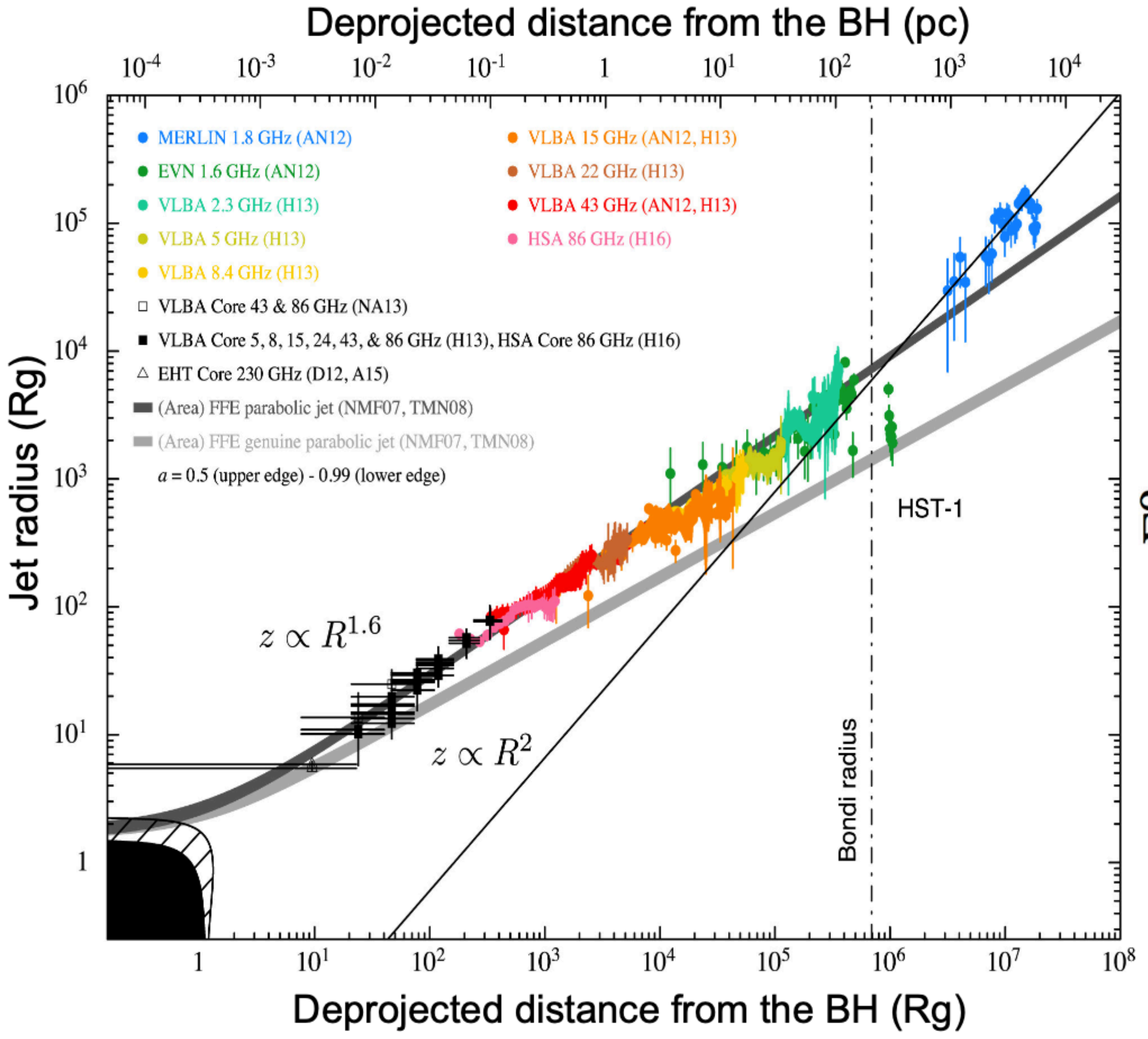

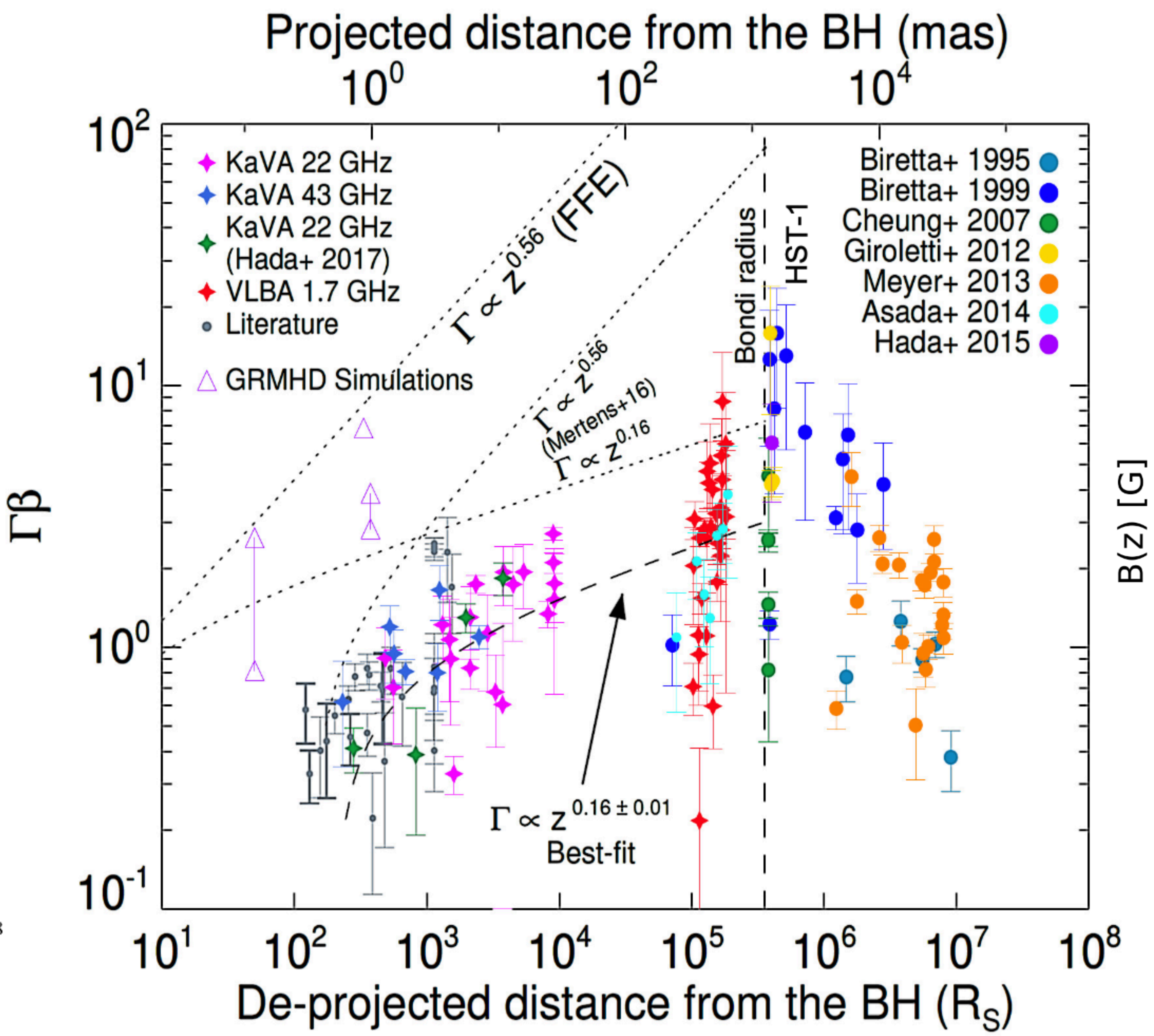

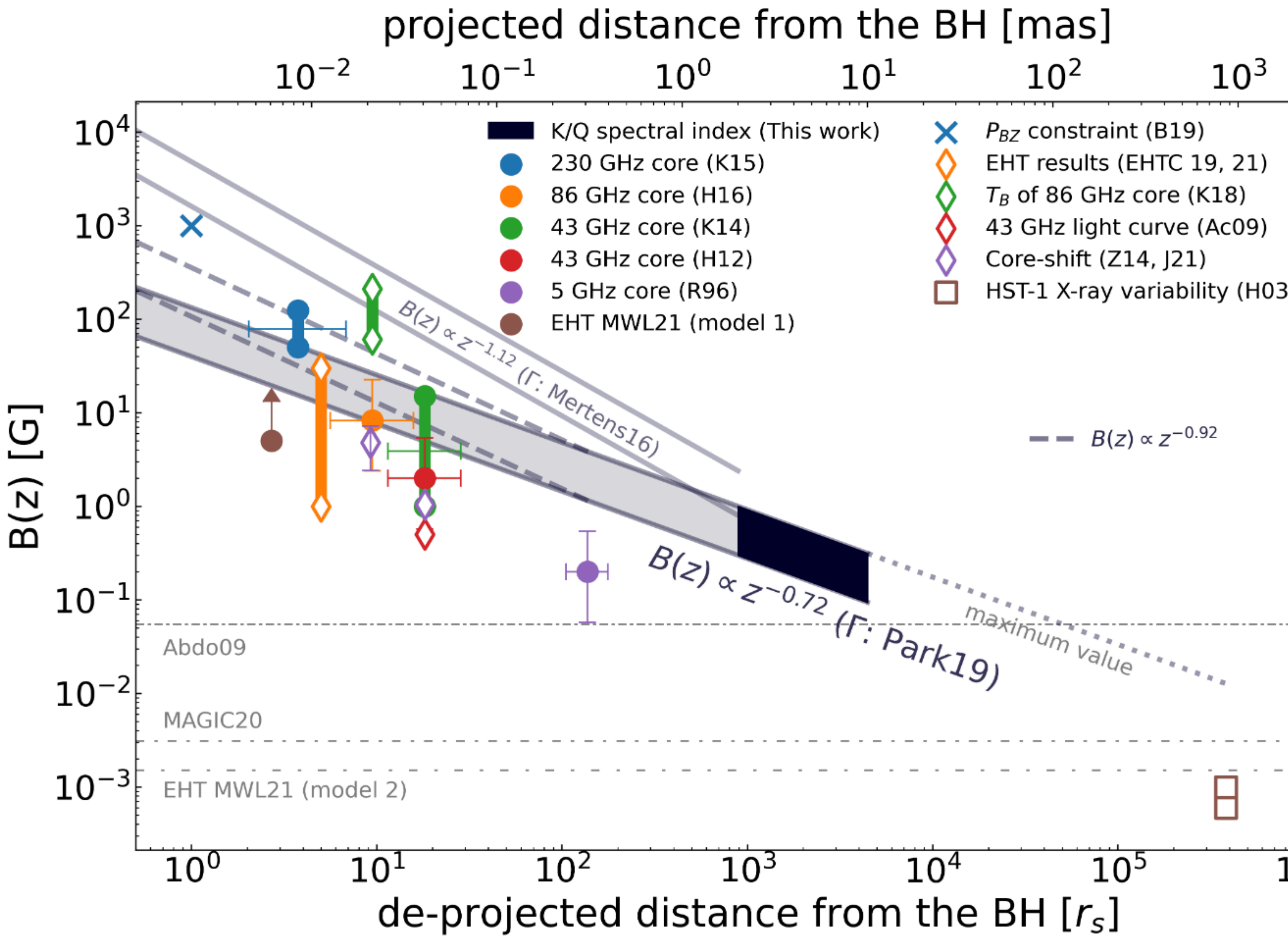

$$R(z) = 1.67 r_g (z/r_g)^{0.625}$$

$$\Gamma_j(z) = 0.8 (z/r_g)^{0.16}$$

$$B'(z) \propto (\Gamma_j R)^{-1} = 80\,(z/r_g)^{-0.785}\,\mathrm{G}$$

Nakamura+ 2018; Park+ 2019;Ro+ 2023

Dominant acceleration process for M87

time scale vs. electron energy for different distance to the black hole (z)

Shear acceleration takes over at larger z

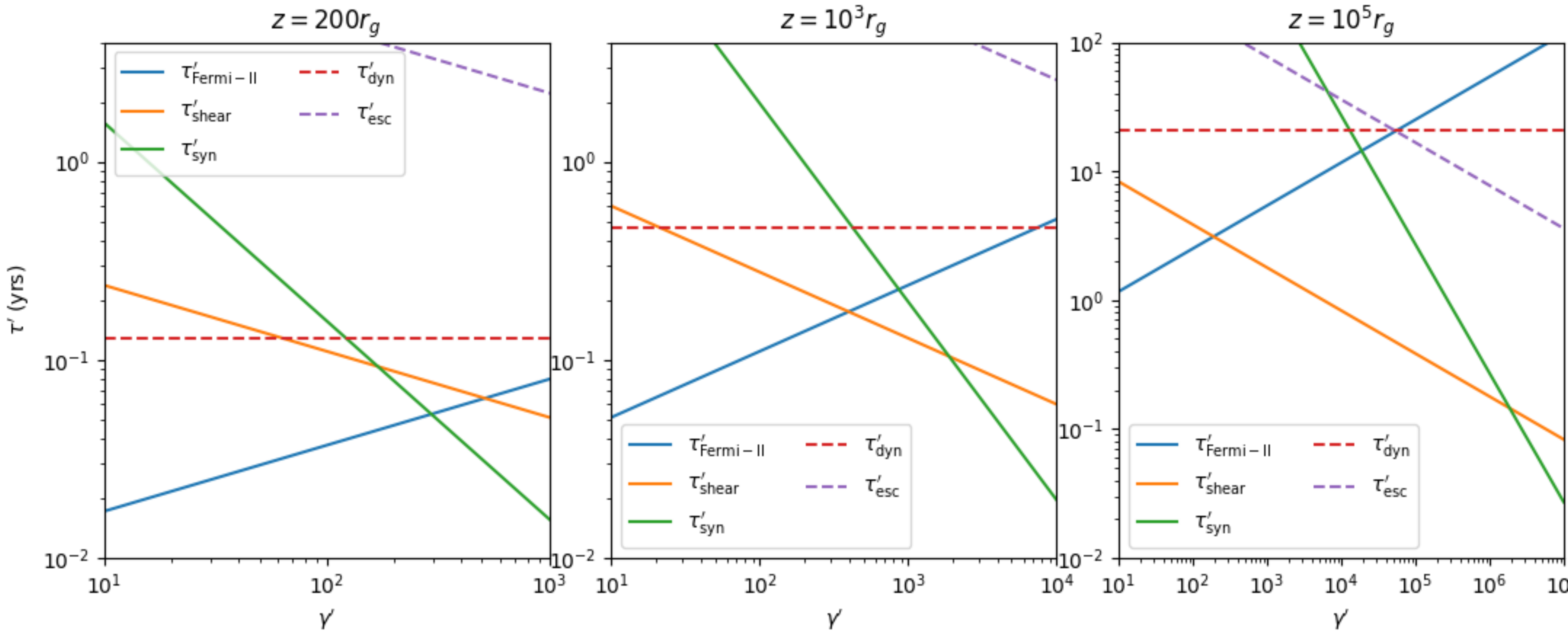

$$\tau'_{\mathrm{Fermi-II}} = 2(2+q)^{-1} c^{3-2q} B'^{q-2} e^{q-2} m_e^{2-q} \gamma'^{2-q} \lambda'^{q-1}_{\mathrm{c}} A'^{-1}_{\mathrm{Fermi-II}} \zeta^{-1}$$

$$\approx 1.5 \times 10^{-4} R_{-2}^{2/3} \gamma'^{1/3} B'^{-1/3}_{-1} \beta'^{-2}_A \zeta^{-1}_{-2} \text{ yrs},$$

$$w = 0.1,\ \beta_A = 0.1$$

$$\tau'_{\mathrm{shear}} = 1.5(6-q)^{-1} w B'^{2-q} e^{2-q} m_e^{q-2} \gamma'^{q-2} R^2 \lambda'^{1-q}_{\mathrm{c}} \zeta,$$

$$= 1.4 \eta R^{4/3}_{-2} B'^{1/3}_{-1} w \zeta_{-2} \gamma'^{-1/3} \text{ yrs},$$

$$\tau'_{\mathrm{sc}} \approx \zeta^{-1} r'^{2-q}_{\mathrm{L}} \lambda'^{q-1}_{\mathrm{c}} c^{-1}$$

J.S.Wang+,2024, arXiv:2404.08625

Application to inner jet of M87

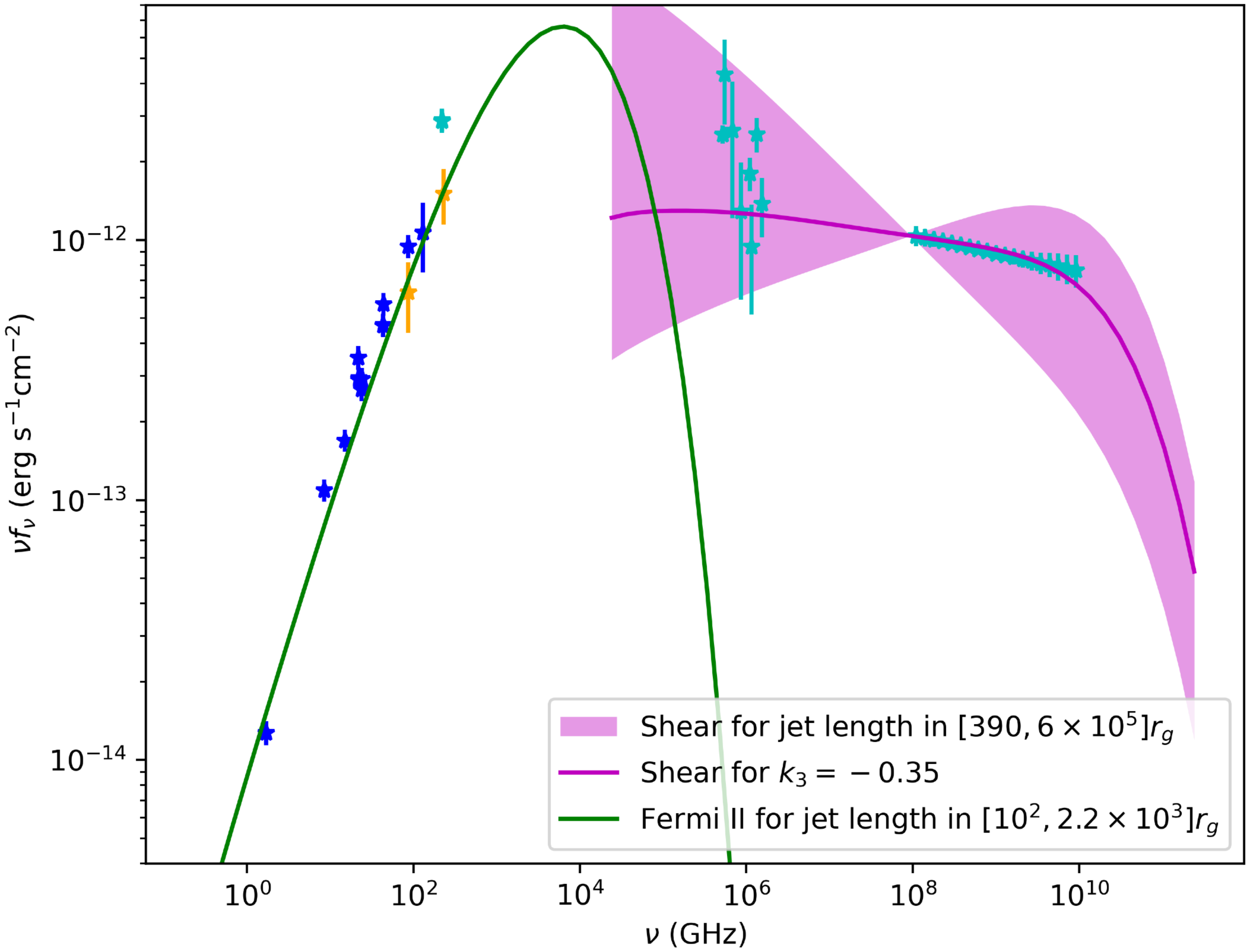

J.S.Wang+, 2024, ApJ, arXiv:2404.08625

$$f_\nu = \int_{z_{\min}}^{z_{\max}} f_\nu(z)dz$$

Integration region determined by the angular resolution at corresponding frequencies

$$f_\nu(z)dz = \delta_{\mathrm{D}}^3(z)S(z)dz\int_{\gamma'_{\min}}^{+\infty} n'(\gamma', z)F_{\mathrm{syn}}(\gamma', \nu')d\gamma'$$

$$\delta_{\mathrm{D}} = [\Gamma_{\mathrm{j}}(1-\beta_{\mathrm{j}}\cos i)]^{-1}$$

Shaded region depends on the number density over distance (z) to the black hole

$$n'(z) \propto z^{k_3}\rho'(z)$$

Application to kpc-scale jet of Cen A

TeV observations by HESS
v~0.6c by radio observations

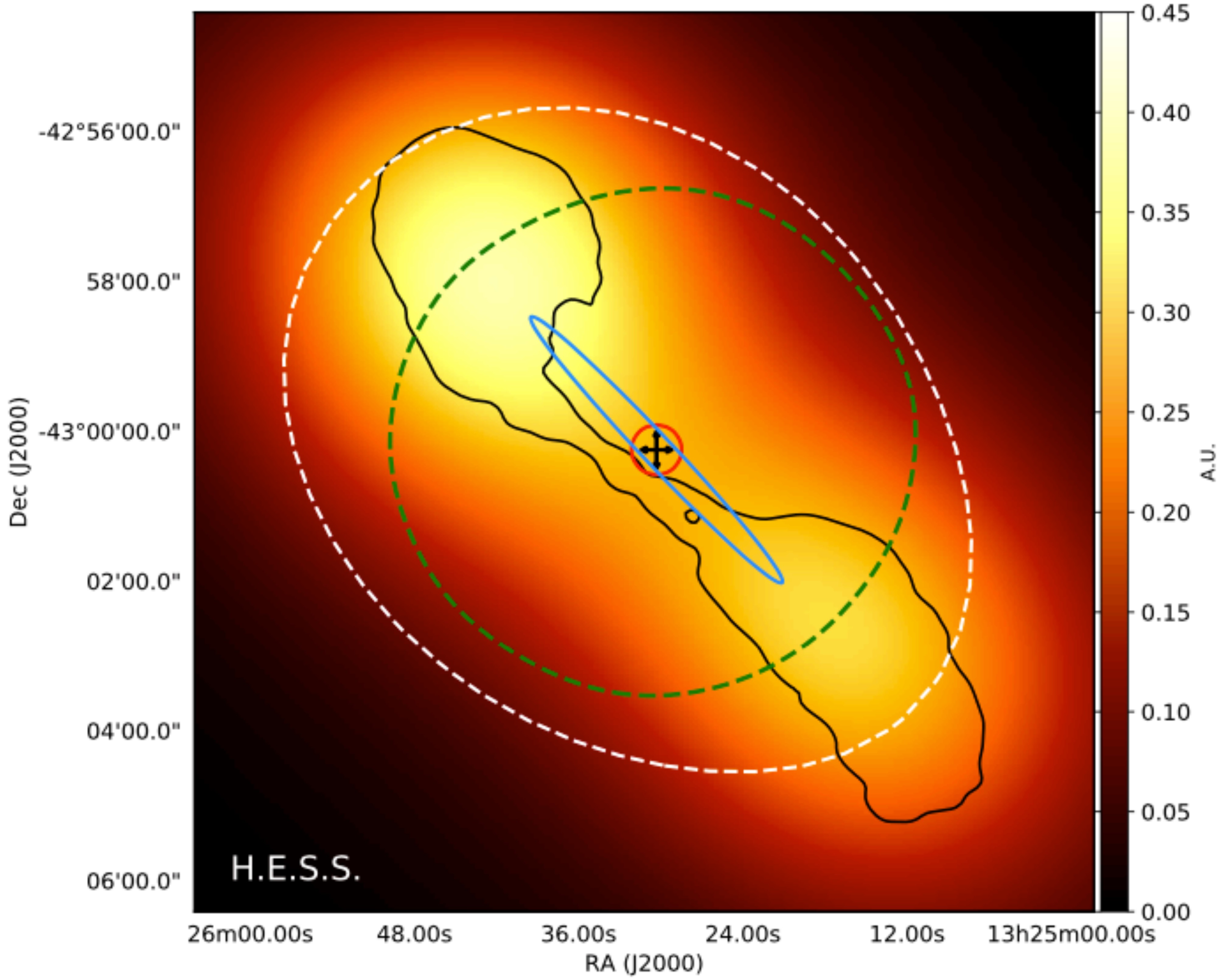

H. E. S. S. Collaboration, 2020, Nature

X-ray and TeV emission explained by shear acceleration

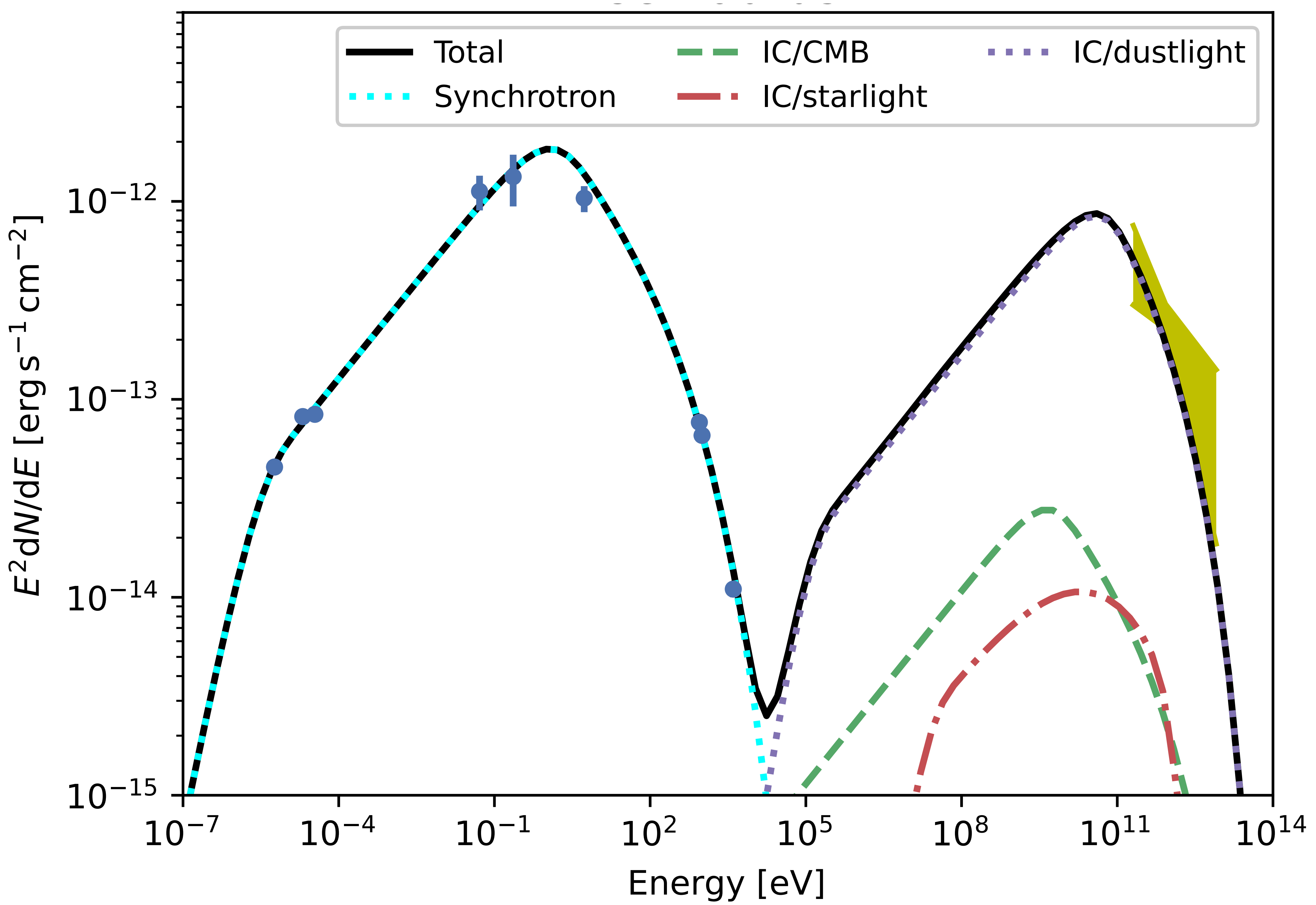

J.S.Wang+, 2021, MNRAS, arXiv:2105.08600

Analytical theory works for observations

↓

Numerical simulations for stochastic-shear acceleration

Relativistic MHD simulations with PLUTO

- Stochastic-shear acceleration depends on turbulence and velocity profile
- Periodic box simulations to study the jet instabilities (e.g. Kelvin-Helmholtz)
- Different parameters from analytical modeling of radio galaxies :

$v \in [0.6, 0.99]c,$

$\sigma \in [0.002, 0.2]$

$\sigma_{y,\phi} = < B^2_{y,\phi} > / 8\pi\rho_0 c^2$

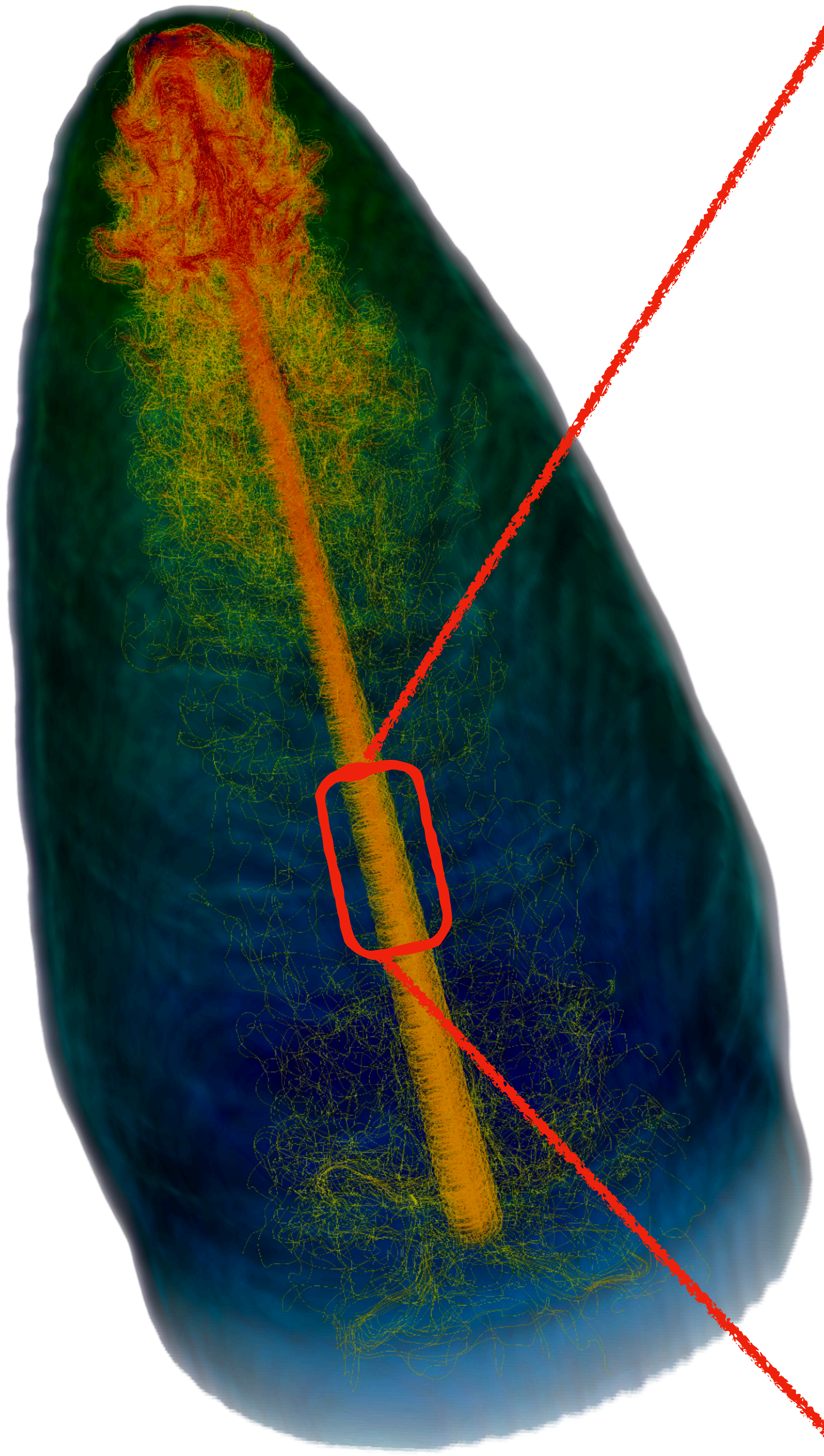

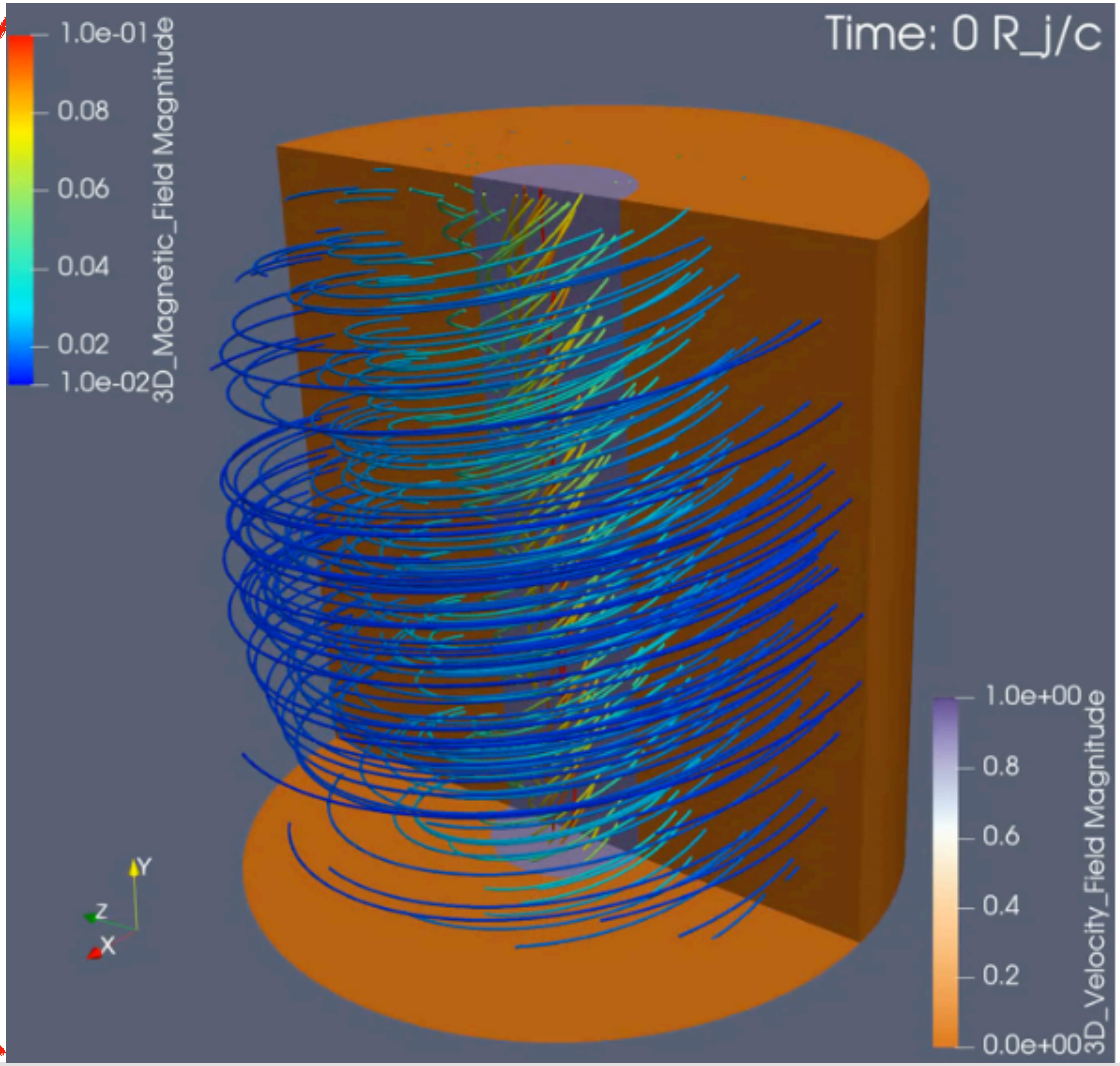

J.S.Wang+, 2023, MNRAS, arXiv:2212.03226

Relativistic MHD simulations with PLUTO

- Stochastic-shear acceleration depends on turbulence and velocity profile
- Periodic box simulations to study the jet instabilities (e.g. Kelvin-Helmholtz)
- Different parameters from analytical modeling of radio galaxies :

$v \in [0.6, 0.99]c,$

$\sigma \in [0.002, 0.2]$

$\sigma_{y,\phi} = < B^2_{y,\phi} > / 8\pi \rho_0 c^2$

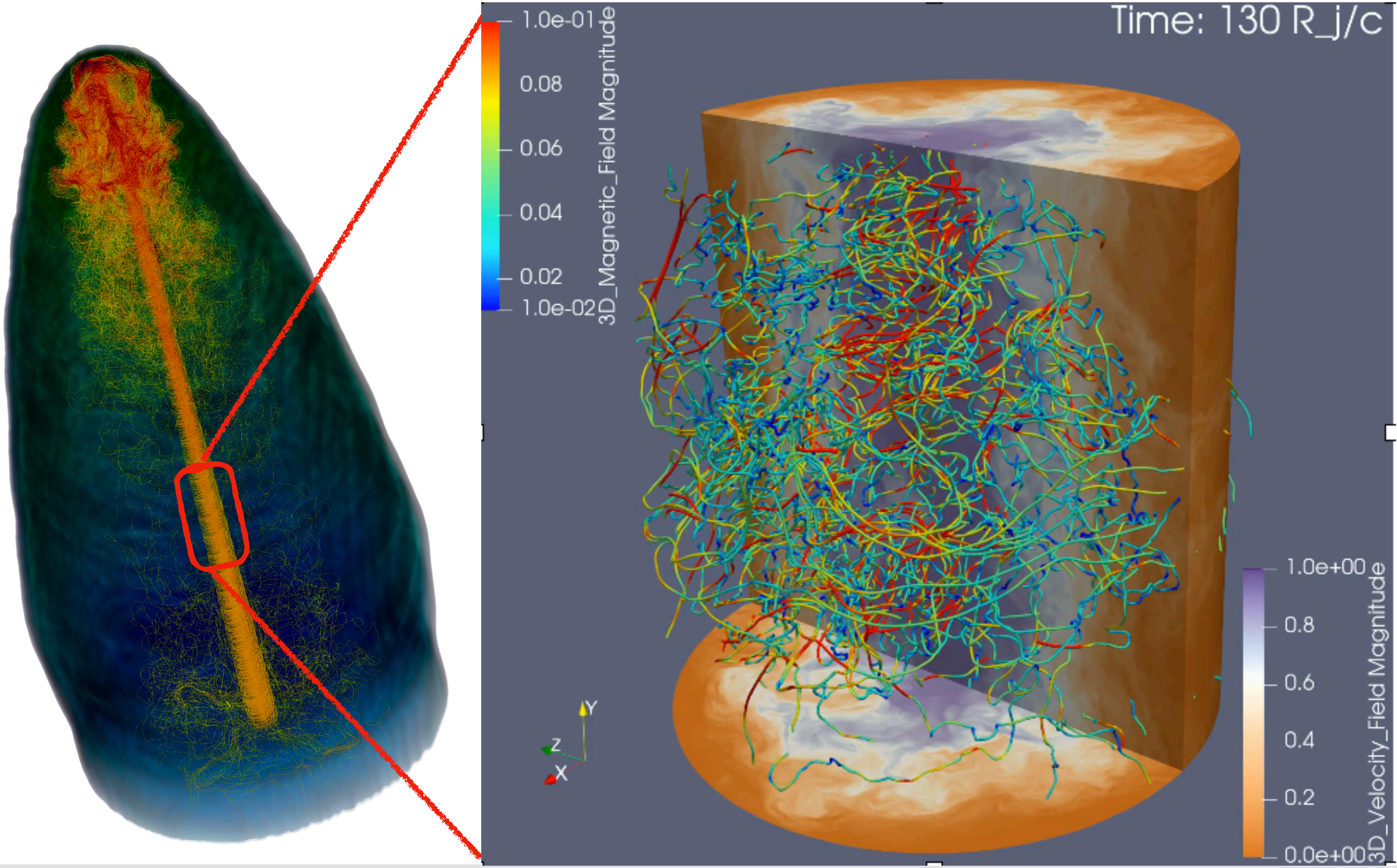

J.S.Wang+, 2023, MNRAS, arXiv:2212.03226

Relativistic MHD + Test-particle Simulations

- Higher-resolution (~1000³) runs without sub-grid physics for test particles

$$R_{\text{domain}} : R_0 : r_{g,\text{inj}} : \Delta x \approx 1000 : 200 : 3 : 1$$

- FR I: (v = 0.6c, R_0 = 0.1kpc)
- FR II: (v = 0.9c, R_0 = 1kpc)
- Magnetization: $\sigma = 0.02,\ 0.2$

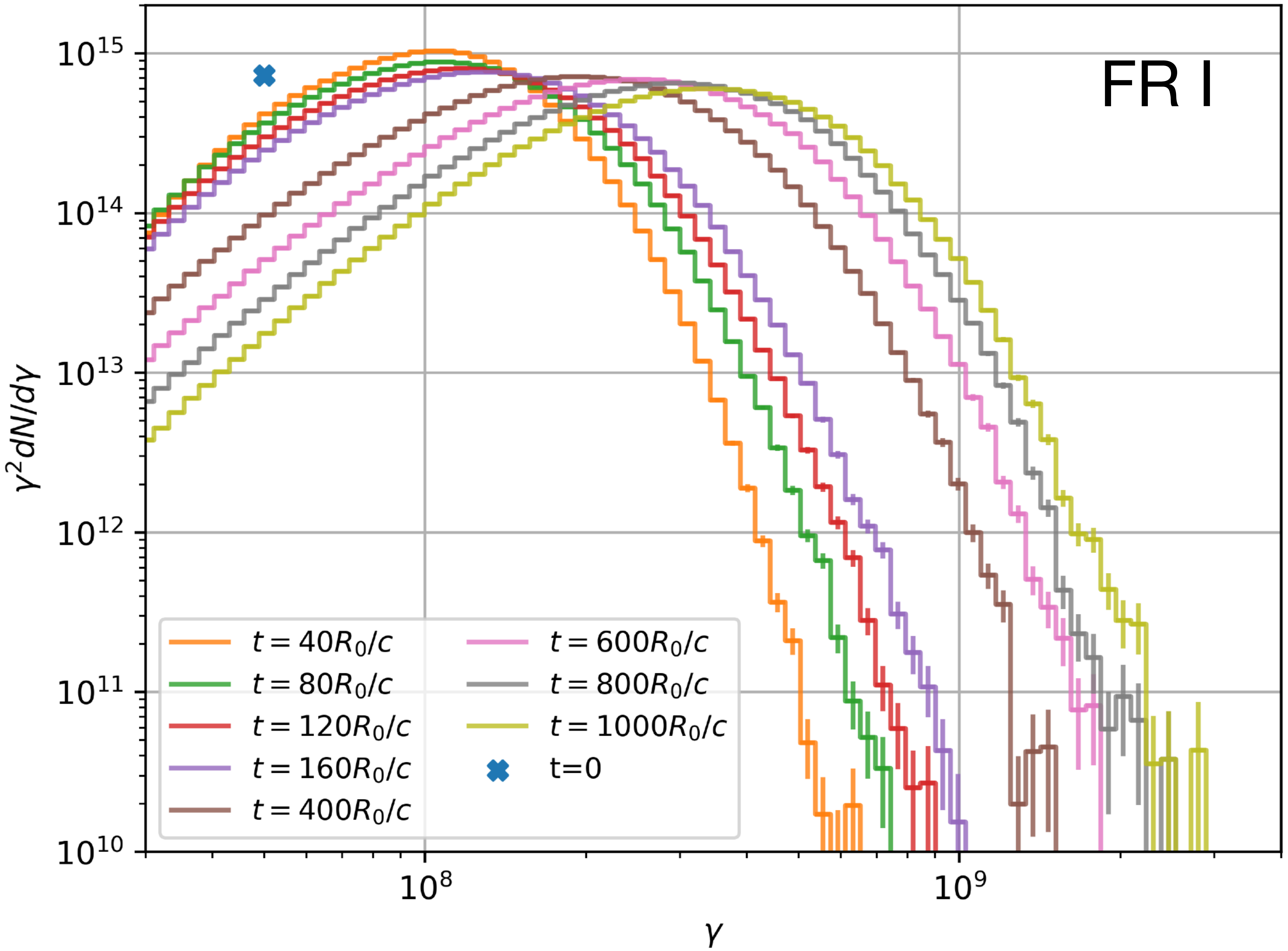

Particle spectrum

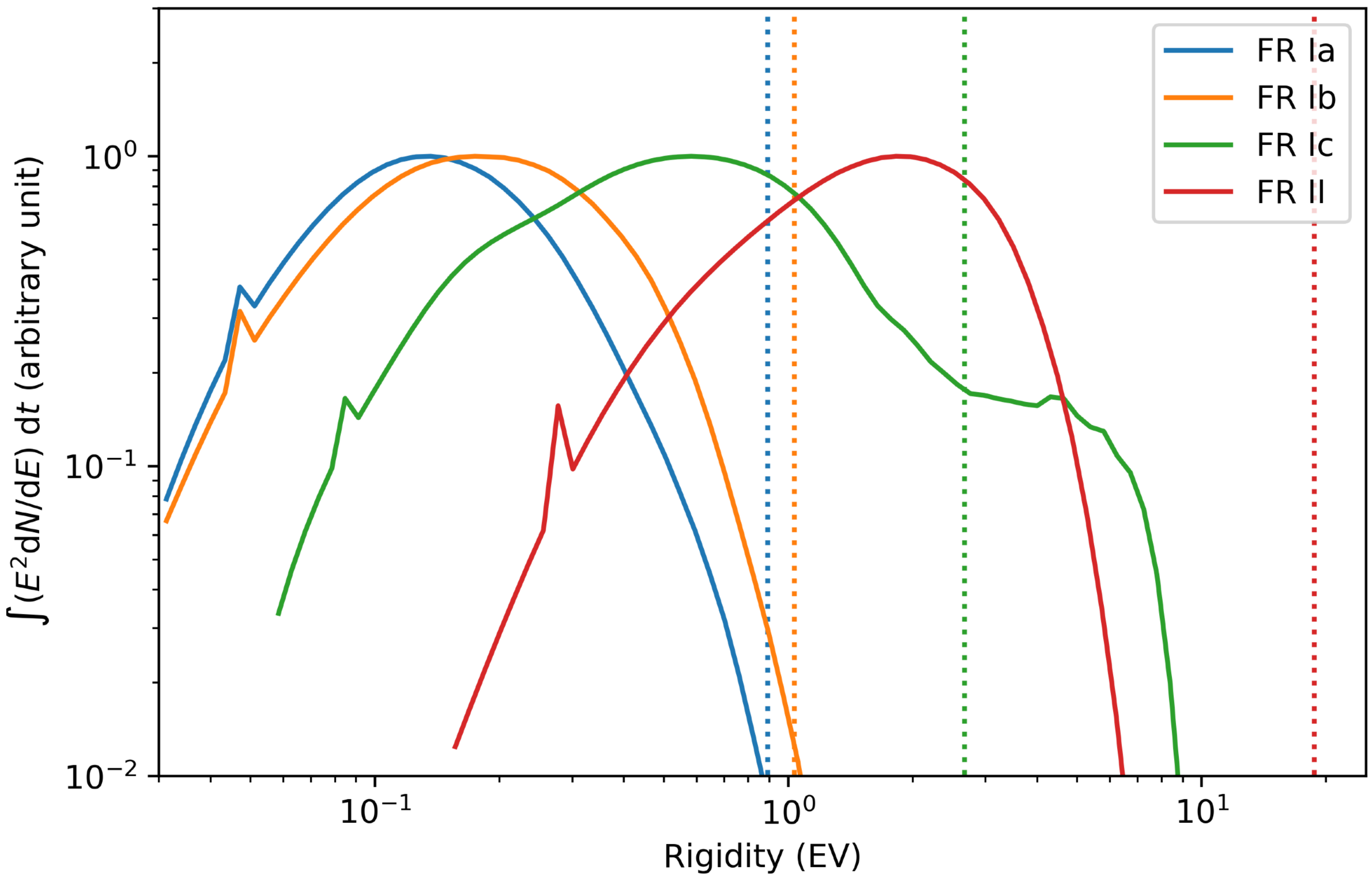

Rigidity= E/Ze

$E_{\rm peak} \approx 0.1 - 0.3\ E_{\rm Hillas}$

$E_{\rm Hillas} \approx Ze\bar{v}\bar{B}R$

for different v and B values

Particles efficiently accelerated close to the maximum theoretical limit (Hillas limit)

Summary

- Stochastic-shear acceleration is an unavoidable (KH instability) and efficient mechanism in relativistic jets
- In the framework of stochastic-shear acceleration, both multi-wavelength observation of M87 inner jet and Cen A jet can be explained
- Cosmic rays can be accelerated to close to the maximum theoretical limit ($E_{\rm peak} \approx 0.1 - 0.3\ E_{\rm Hillas}$), and large-scale AGN jet can contribute to CRs above EeV